Prediction of Sound Fields in Cavities with Sound Absorbing Materials

Hideo Utsuno,* Ting W. Wu,† and Andrew F. Seybert‡
University of Kentucky, Lexington, Kentucky 40506
and
Toshimitsu Tanaka§
Kobe Steel, Ltd., Kobe, 673-02, Japan

A sound field in a three-dimensional cavity containing sound absorbing materials was studied using the boundary element method. The sound absorbing material was considered as bulk reacting, and its effective density and propagation speed were measured by a technique based on the transfer function method. Two cavity models were utilized to assess the accuracy of calculation: one was a cavity with a bulk of sound absorbing material within the interior, and the other was a larger cavity divided into two smaller cavities by a panel of the sound absorbing material. Frequency response curves, resonance frequencies, and damping ratios calculated for the cavity models were compared with experimental ones. The excellent agreement achieved suggests that the present method is sufficiently reliable to predict the acoustic properties of the sound field in a cavity containing bulk-reacting sound absorbing materials.

Introduction

NUMEROUS studies have been conducted into the problem of how to decrease the interior noise level in aircraft and automobiles, as was shown in a survey paper by Dowell.[1] The present paper focuses on the prediction of sound fields in a cavity containing sound absorbing materials, which has been of practical importance and needs additional investigation.

The prediction of acoustic resonance frequencies for an arbitrarily shaped cavity geometry has been reasonably successful due to the progress of high-speed digital computers in recent years. Shuku and Ishihara[2] reported good agreement between calculations and experiments for two-dimensional automobile compartments using the finite element method (FEM). Similar good results were also reported by several other researchers,[3-5] provided that the cavity is surrounded by rigid walls. However, the prediction of sound fields with sound energy dissipation is of practical interest; for example, a vehicle contains seats and carpets that dissipate sound energy.

Based on their characteristics, sound absorbing materials may be divided into two groups: locally reacting and bulk reacting.[6] The former are characterized by a normal acoustic impedance valid at the material surface. In the latter, the sound absorbing material itself is considered as a medium transmitting sound waves, and it is characterized by the complex propagation speed and the complex effective density.

Some excellent studies of the sound field with sound absorbing materials have been conducted to analyze dissipative mufflers lined with sound absorbing materials. Assuming the material is bulk reacting, Scott[7] analytically studied a lined duct transmitting plane waves. Astley and Cummings[8] reported good agreement between calculations and experiments for three-dimensional dissipative ducts by using the FEM, utilizing the bulk reacting properties obtained empirically. Terao and Sekine[9] applied the boundary element method (BEM) to the prediction of sound in a two-dimensional dissipative duct after they directly measured the bulk-reacting properties using both the transfer function method[10,11] and the two-thickness method[12] together.

On the other hand, in problems involving cavities with sound absorbing materials, Craggs[13] studied small rooms lined with bulk-reacting materials using the FEM. Assuming locally reacting materials, Bernhard et al.[14] applied the BEM to aircraft interior cavities and Utsuno et al.[15] applied the BEM to automobile compartments. Seybert et al.[16] used the BEM to model lined, partially open enclosures. Suzuki et al.[17] studied the sound fields in a cavity with complicated boundary conditions.

However, further studies are needed to predict the acoustic properties of the sound field in a cavity containing sound absorbing materials. The objective of this paper is to show how the three-dimensional sound field in a cavity with bulk-reacting sound absorbing materials can be studied using the BEM and to assess the accuracy of the calculation by comparison with experiments.

In this paper, the multidomain boundary element program BEMAP[18,19] was used to predict the sound field in a cavity with sound absorbing materials. The characteristics of the sound absorbing materials utilized were measured by using the improved two-cavity method.[20] Two cavity models were studied: one was a cavity with a bulk of sound absorbing material within the interior, and the other model consisted of two cavities separated by a panel of sound absorbing material. The acoustic properties of both models, including frequency response curves, resonance frequencies, and damping ratios were calculated and compared with experiments.

Boundary Element Method

Formulation of the Method

Several formulations of the BEM[21,22] have been derived to be applied to an acoustical interior problem. The multidomain formulation[18] may be derived by considering two domains, Ω_1 and Ω_2, separated by an interface, as depicted in

Received July 10, 1989; revision received Oct. 30, 1989.

*Visiting Scholar, Department of Mechanical Engineering; Researcher, Kobe Steel, Ltd.
†Assistant Professor, Department of Mechanical Engineering.
‡Professor, Department of Mechanical Engineering.
§Senior Researcher, Mechanical Engineering Research Laboratories.

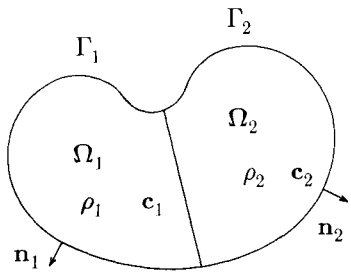

Fig. 1 Schematic diagram of a two-domain problem.

Fig. 1. In each domain, the Helmholtz equation is satisfied:

$$\nabla^2\phi_1 + k_1^2\phi_1 = 0 \qquad \text{in } \Omega_1 \tag{1}$$

$$\nabla^2\phi_2 + k_2^2\phi_2 = 0 \qquad \text{in } \Omega_2 \tag{2}$$

where ϕ_1 and ϕ_2 are the velocity potential for each domain and k_1 and k_2 are the wave numbers in each domain, respectively. For each acoustical domain, a boundary integral equation can be obtained:

$$C_1(P)\phi_1(P) = \int_{\Gamma_1}\left(\psi_1\frac{\partial\phi_1}{\partial n_1} - \phi_1\frac{\partial\psi_1}{\partial n_1}\right)d\Gamma_1 \tag{3}$$

$$C_2(P)\phi_2(P) = \int_{\Gamma_2}\left(\psi_2\frac{\partial\phi_2}{\partial n_2} - \phi_2\frac{\partial\psi_2}{\partial n_2}\right)d\Gamma_2 \tag{4}$$

where Γ is the boundary surface for the domain, including the interface, n is the unit normal on Γ directed away from Ω, and the subscripts 1 and 2 refer to the quantities in domains 1 and 2, respectively. The function ψ is the free-space Green function $\psi = \exp(-jkr)/r$, in which $r = |P - Q|$, where Q is any point on Γ, and P may be in Ω, Ω', or on Γ, where Ω' is the domain exterior to Ω. The coefficient $C(P)$ has the value 4π for P in Ω, 0 for P in Ω', and 2π for P on Γ, provided there is a unique tangent plane to Γ at such a P. A more general form of $C(P)$ valid for arbitrary geometry (e.g., edges or corners) is given in Ref. 18.

At the interface where the domains are adjacent, the solution is governed by the following continuity constraints:

Continuity of the normal velocity:

$$\frac{\partial\phi_1}{\partial n_1} = -\frac{\partial\phi_2}{\partial n_2} \tag{5}$$

Continuity of the acoustic pressure:

$$\rho_1\phi_1 = \rho_2\phi_2 \tag{6}$$

where ρ_1 and ρ_2 are the effective densities of the media in domains 1 and 2, respectively.

Using a boundary element discretization procedure,[18] the integral equations for each domain are reduced to a matrix form:

$$[A]\boldsymbol{x} = b \tag{7}$$

where the vector $\boldsymbol{x}$ contains the unknowns on the boundary and on the interface. By solving Eq. (7), the unknown boundary and interface values can be obtained.

Test Case: Numerical Implementation for a Straight Duct

To verify the numerical procedure, the acoustic field in a straight duct excited by a flat piston at one end and terminated by a rigid wall at the other, as shown in Fig. 2, was studied. The numerical solution was compared with an analytical plane-wave solution. The medium in domains Ω_1 and Ω_3 is air, and a sound absorbing material is contained in domain Ω_2. It was assumed that the effective density $\rho_2 = 7 - 10j$ kg/m^3, the propagation speed $c_2 = 100 + 40j$ m/s, and both are independent of frequency. The sound pressure P (Pa) at the piston surface was calculated over a frequency range below 1000 Hz when the piston was excited to provide a uniform velocity distribution , $V = 1$ m/s. In the BEM calculation, the domains Ω_1 and Ω_3 were discretized into 0.1-m squares by using quadratic elements. The ratio of element size to wavelength at 1 kHz is about 0.3 in domains Ω_1 and Ω_3. The domain Ω_2 was discretized finer than the domains Ω_1 and Ω_3 because the sound wave generally transmits slower in the sound absorbing material than in air. The element is 0.03 m in length along the duct axis in domain Ω_2. The ratio of element size to wavelength at 1 kHz is also about 0.3 in domain Ω_2. The frequency response curve 20 log(P/V) is shown in Fig. 3, where the solid line represents a plane-wave analytical solution obtained by the transfer matrix method and the open squares represent the BEM calculation. An excellent agreement between the analytical solution and the BEM calculation can be seen.

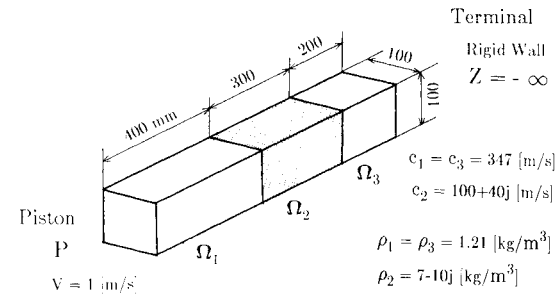

Fig. 2 A straight duct containing a sound absorbing material.

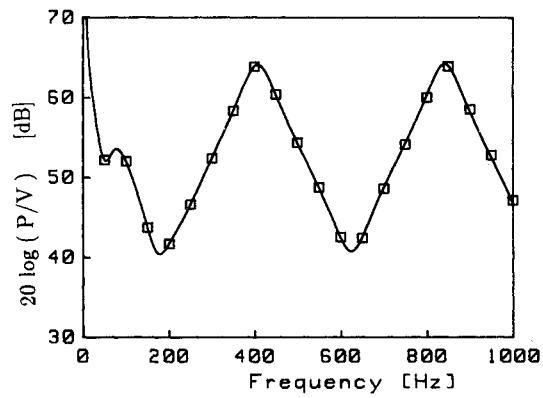

Fig. 3 Frequency response curve of sound pressure at piston surface: —— analytical solution; □ BEM calculation.

Sound Absorbing Material

Measurements by the Improved Two-Cavity Method

The complex propagation speed c and the complex effective density ρ of a homogeneous sound absorbing material were measured by means of the improved two-cavity method.[20] This method needs only one test piece, therefore, the characteristic of the test piece can be measured more accurately than by means of the two-thickness method,[9] which needs two test pieces. The variation of the material between two test pieces and the variation associated with test piece mounting in the two-thickness method can be eliminated in the improved two-cavity method.

An experimental apparatus is shown in Fig. 4. The thickness of the test material is d, the air space depth behind the material is L, the acoustic impedance measured at the material surface is Z_0, and the acoustic impedance behind the

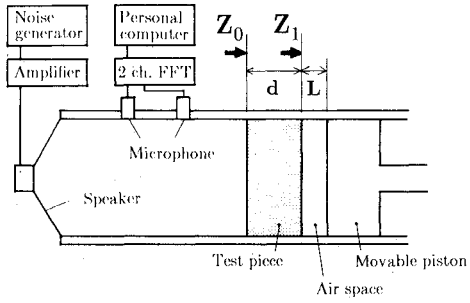

Fig. 4 Block diagram of the improved two-cavity method.

material is Z_1. In the calculation, prime ('), represents the quantities obtained at another air space depth L'. The characteristic impedance ρc and the propagation speed can be related to Z_0, Z_0', Z_1, and Z_1', as follows[20]:

$$\rho c = \pm\left[\frac{Z_0 Z_0'(Z_1 - Z_1') - Z_1 Z_1'(Z_0 - Z_0')}{(Z_1 - Z_1') - (Z_0 - Z_0')}\right]^{1/2} \tag{8}$$

$$c = -2j\,\mathrm{d}\omega/\ell n\left(\frac{Z_0 - \rho c}{Z_0 + \rho c}\frac{Z_1 + \rho c}{Z_1 - \rho c}\right) \tag{9}$$

where the sign in Eq. (8) is selected so as to let the real part of of ρc be positive. The acoustic impedance Z_0 and Z_0' can be obtained experimentally using the transfer function method,[10,11] and Z_1 and Z_1' are obtained analytically, as follows:

$$Z_1 = -jZ_{\text{air}}\cot(kL) \tag{10}$$

$$Z_1' = -jZ_{\text{air}}\cot(kL') \tag{11}$$

where k is the wave number of air and Z_{air} is the characteristic impedance of the air. Substituting Z_0, Z_0', Z_1, and Z_1' into Eqs. (8) and (9), ρ and c can be calculated.

Characteristics of Sound Absorbing Material

Two different test materials were used in the experiment. One was glass fiber and the other a urethane foam. The names and the measuring conditions are shown in Table 1. Three test pieces were cut out of the same sheet of the material, and the characteristics of that material were measured six times from both the front and the rear so that any variation that may exist among the test pieces could be determined.

The six propagation speeds of the glass fiber and the urethane foam are shown in Figs. 5a and 5b, respectively. The six effective density of the glass fiber and the urethane foam are shown in Figs. 6a and 6b, respectively. Although there are slight deviations, a consistent trend can be observed. For this reason, the characteristics of the sound absorbing material were represented by the average value of these six recordings.

Experimental Apparatus of Cavity Model

The experimental cavity model used in this investigation is shown in Fig. 7. It consists of a large box and a short inlet duct. The overall dimensions of the box are 306-mm long, 255-mm wide, and 204-mm high; those of the inlet duct are 55-mm long, 51-mm wide, and 51-mm high. Both were made of 20-mm-thick acrylic plastic. Two holes were drilled in the walls at locations 1 and 2 in order to measure the sound

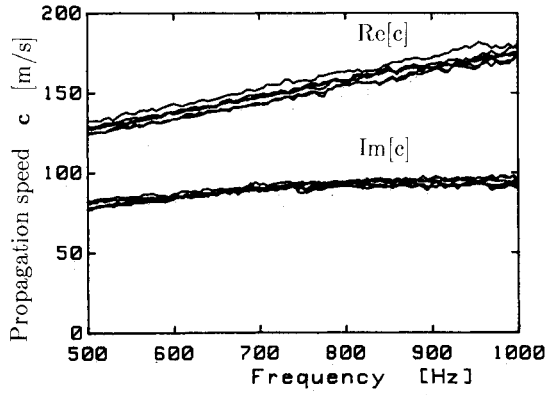

Fig. 5a Six propagation speeds of glass fiber.

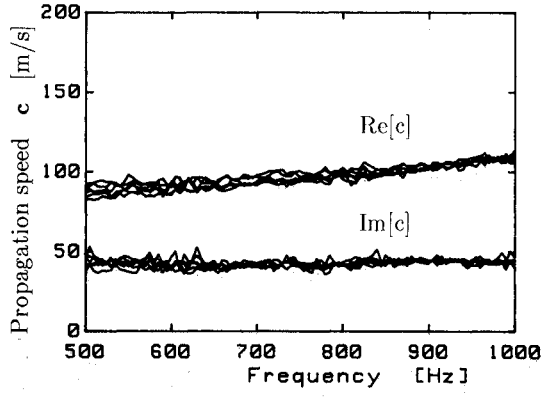

Fig. 5b Six propagation speeds of urethane foam.

pressure. The entrance to the inlet duct contained a 20-mm-thick acrylic plastic piston, which could be moved by a vibration exciter along the x axis, as depicted in Fig. 8. The space between the piston and the inlet duct walls was sealed by vinyl film, so that any sound radiated from the piston would not leak through and the vibration of the piston would not transmit to the inlet duct wall. With the piston driven with a white noise vibration, the vibration velocity of the piston V (m/s) and the sound pressure P (Pa) at location 1 or 2 were measured and the transfer function 20 log (P/V) was determined using a two-channel fast Fourier transform analyzer.

Results and Discussion

Two different cavity configurations were used to study the effect of the sound absorbing materials. In one, the cavity was separated by a sound absorbing material, whereas, in the other, a bulk of a sound absorbing material was suspended within the interior of the cavity, like a seat in a vehicle passenger compartment.

In the BEM calculation, c and ρ for air were taken as 347 m/s and 1.21 kg/m^3, respectively; whereas, in the domain occupied by the test material, the averages of the measured characteristics shown in Fig. 5 or 6 were used. On the boundary elements corresponding to the piston surface, a

Table 1 Sound absorbing materials and measuring conditions

Test material	Name	Maker	d, mm	(L, L'), mm
Glass fiber	232500	Nippon Mineral Fiber	50	(10, 20)
Urethane foam	VO foam	Bridgestone	50	(10, 20)

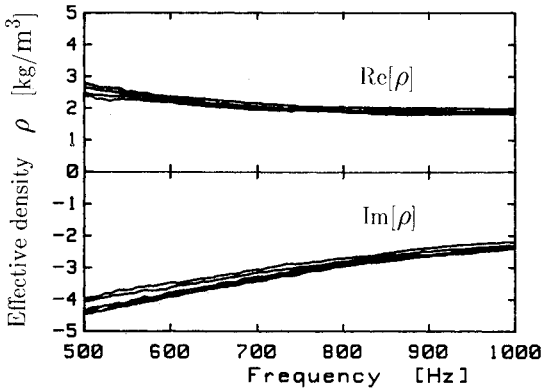

Fig. 6a Six effective densities of glass fiber.

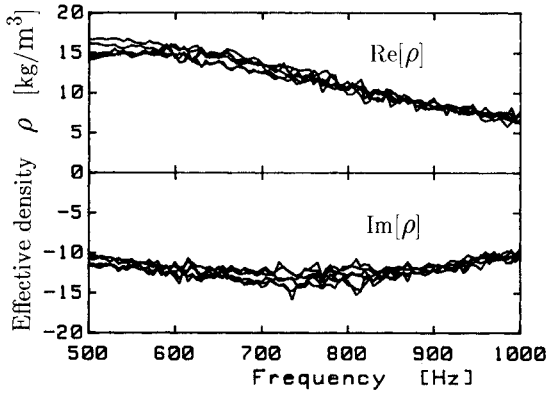

Fig. 6b Six effective densities of urethane foam.

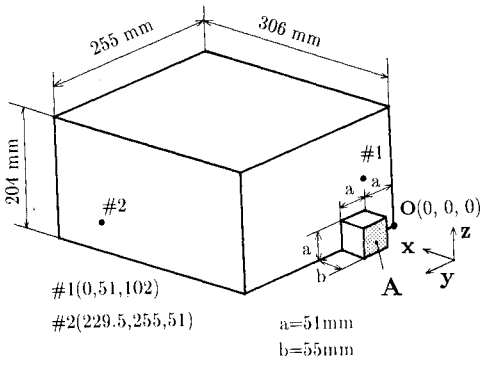

Fig. 7 Three-dimensional sound field in a cavity.

uniform vibration velocity $V = 1$ m/s was assumed and all other surfaces except for the piston were assumed to be rigid.

For the first cavity configuration, there were three domains: two were occupied by air and separated by the third which consisted of a 50-mm-thick layer of sound absorbing material, as shown in Fig. 9. Two tests were run using the first cavity configuration. In one test, the sound absorbing material was the glass fiber material, and, in the second test, the urethane foam was used as the sound absorbing material.

The surfaces of the three domains were discretized using quadrilateral boundary elements. All boundary elements were 76.5-mm long in the x direction and approximately 50-mm long in each of the y and z directions. The total number of elements and nodes were 180 and 546, respectively. As the recommended element size for quadratic elements is one-half wavelength, and the smallest wavelength occurs in the urethane foam where the speed of sound is less than one-third

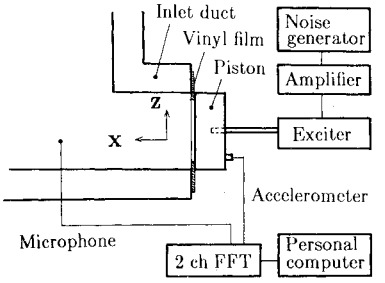

Fig. 8 Block diagram of the experimental measuring apparatus.

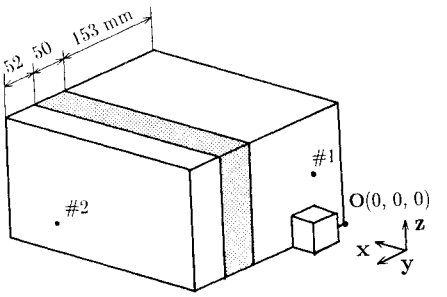

Fig. 9 Sound field in cavities separated by a panel of sound absorbing material.

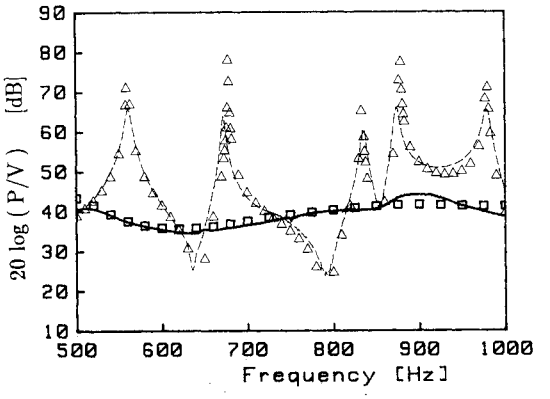

Fig. 10a Frequency response curve for the cavity model shown in Fig. 9 for measurements taken at location 1: □ BEM calculation with glass fiber; —— experiment with glass fiber; △ BEM calculation without glass fiber; - - - experiment without glass fiber.

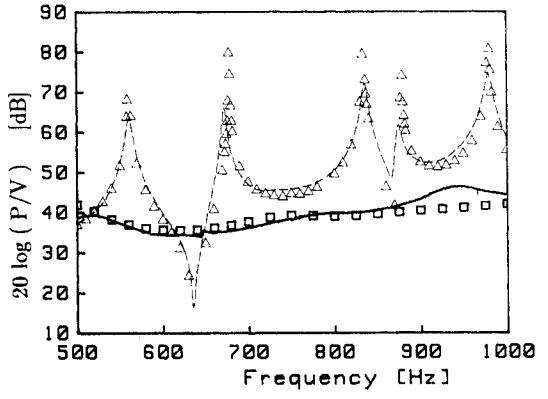

Fig. 10b Frequency response curve for the cavity model shown in Fig. 9 for measurements taken at location 2: □ BEM calculation with glass fiber; —— experiment with glass fiber; △ BEM calculation without glass fiber; - - - experiment without glass fiber.

the value in air, the BEM calculation was carried out at frequencies up to 1000 Hz.

The frequency response curve 20 log (P/V) at location 1 is shown in Fig. 10a. The frequency range from 500 Hz to 1 kHz is the main interest here as it contains the first five cavity resonances. In Fig. 10a, the open squares represent the calculated values for the BEM model with glass fiber as the test material and the solid line represents the measured values. The open triangles represent the calculated values for the BEM model with no test material and the broken line represents the measured values. Excellent agreement can be seen for the model with no sound absorbing material. It can also be seen that there is excellent agreement between the calculated and experimental values when the cavity contains glass fiber. In this cavity configuration, the dominant acoustic resonances are suppressed by the sound absorbing material and there appears to be a relatively constant frequency response at location 1.

Figure 10b shows the frequency response curve at location 2, where the sound measured is that which has been transmitted through the test material. Excellent agreement between the measured and calculated values can also be seen.

The frequency response curves at location 1, when the urethane foam was used, are shown in Fig. 11. It can be seen that there is also an excellent agreement for urethane foam.

The second cavity configuration studied is shown in Fig. 12. The sound absorbing material suspended in the cavity was a rectangular parallelpiped with dimensions $153 \times 100 \times 50$ mm. The corner Q of the rectangular parallelpiped was located at $x = 75$ mm, $y = 43$ mm, and $z = 100$ mm. The test material was positioned so that every surface was parallel to that of the acrylic plastic box. The model was discretized as fine as the model shown in Fig. 9; the total number of elements and nodes were 160 and 486, respectively.

Figure 13 shows the frequency response curve for measurements taken at location 2, with and without glass fiber. In Fig. 13, the solid line, open square, and broken line represent the measured values with glass fiber, the calculated values with glass fiber, and the measured values without glass fiber, respectively. Comparing the experimental results with and without glass fiber, it may be seen that there are shifts in the resonance frequencies and a significant decrease of the amplitude at resonance. This is especially noticeable at the third resonance at 837 Hz, which was suppressed so heavily that the dominant peak could no longer be observed. A comparison between the calculated and experimental values showed good agreement in the general shape of the curve, and it may be concluded that the shifts in the resonance frequencies and the absolute amplitudes at resonance were predicted reasonably well.

Figure 14 shows the frequency response curve at location 2, with and without urethane foam. Good agreement between calculated and experimental values may be seen.

The resonance frequencies and damping ratios are shown in Tables 2 and 3. The damping ratios were obtained from the resonance frequencies and the frequencies of the half-power points. The resonance frequencies f_c and f_m represent the calculated and measured values for the cavity configuration with sound absorbing material, respectively. The resonance frequencies f'_c and f'_m represent the calculated and measured values without sound absorbing material. From Tables 2 and 3, it can be seen that the resonance frequencies of the sound field with glass fiber or urethane foam can be predicted to within an accuracy of 1% error using the BEM.

There exists a damping of approximately 0.4% for the cavity without sound absorbing material. For this reason, the measured damping ratio ζ_m consists of both the original damping ζ'_m and the damping due to the test material. Assum-

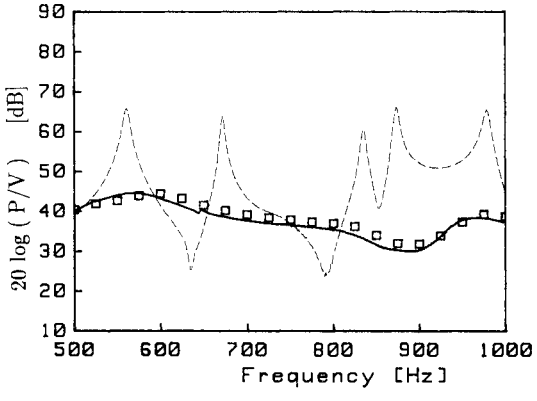

Fig. 11 Frequency response curve for the cavity model shown in Fig. 9 for measurements taken at location 1: □ BEM calculation with urethane foam; —— experiment with urethane foam; – – – experiment without urethane foam.

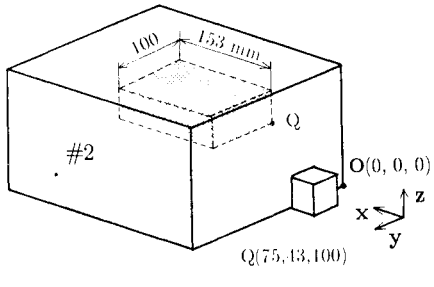

Fig. 12 Sound field in a cavity with a bulk of test material positioned within the interior.

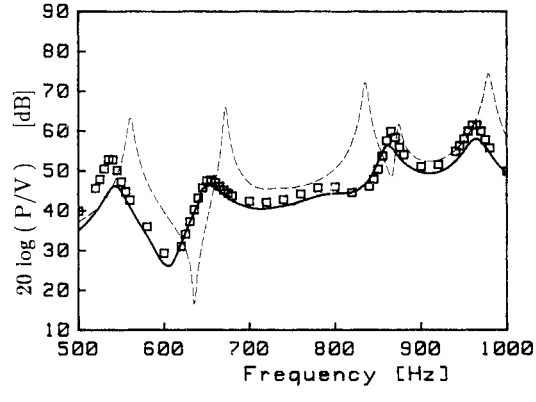

Fig. 13 Frequency response curve for the cavity model shown in Fig. 12 at location 2: □ BEM calculation with glass fiber; —— experiment with glass fiber; – – – experiment without glass fiber.

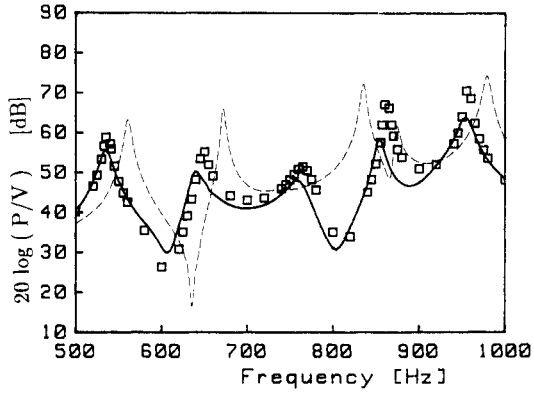

Fig. 14 Frequency response curve for the cavity model shown in Fig. 12 at location 2; □ BEM calculation with urethane foam; —— experiment with urethane foam; – – – experiment without urethane foam.

Table 2 Acoustic properties of sound field with glass fiber

	Resonance frequency, Hz				Damping ratio			
	With fiber		Without fiber		With fiber		Without fiber	
Mode	f_c	f_m	f'_c	f'_m	ζ_c	ζ_m	$(\zeta_m - \zeta'_m)$	ζ'_m
1	538	542	561	561	0.014	0.021	(0.015)	0.0058
2	654	654	678	673	0.023	0.022	(0.019)	0.0033
3	—	—	834	836	—	—	—	0.0036
4	865	863	878	876	0.0079	0.013	(0.0090)	0.0036
5	963	964	979	979	0.011	0.015	(0.011)	0.0039

Resonance frequency and damping ratio obtained by calculation and experiment for the cavity model shown in Fig. 12.

Table 3 Acoustic properties of sound field with urethane foam

	Resonance frequency, Hz				Damping ratio			
	With foam		Without foam		With foam		Without foam	
Mode	f_c	f_m	f'_c	f'_m	ζ_c	ζ_m	$(\zeta_m - \zeta'_m)$	ζ'_m
1	537	535	561	561	0.0067	0.013	(0.0072)	0.0058
2	649	643	678	673	0.0079	0.014	(0.011)	0.0033
3	765	758	834	836	0.015	0.018	(0.014)	0.0036
4	862	855	878	876	0.0019	0.0059	(0.0023)	0.0036
5	957	954	979	979	0.0031	0.0088	(0.0049)	0.0039

Resonance frequency and damping ratio obtained by calculation and experiment for the cavity model shown in Fig. 12.

ing that the damping due to the test material can be added to the original damping, the subtraction $\zeta_m - \zeta'_m$ (the damping of test material itself) is shown in Tables 2 and 3 in parentheses. When this value is compared with the calculated value ζ_c, it can be seen that both are nearly the same for all cases. If more care is taken in conducting the experiment to reduce the original damping, the measured value will be in better agreement with the calculated value. Therefore, it can be concluded that the effect of a sound absorbing material may be predicted with good accuracy.

Summary

A method for analyzing the sound field in a cavity with sound absorbing materials was studied by using the BEM. The characteristics of the sound absorbing material, determined by means of the improved two-cavity method, were utilized. Glass fiber and urethane foam were used as the test materials. The sound fields studied were two cavities separated by a panel of test material and a cavity containing a bulk of test material suspended within the interior. Excellent agreement in the frequency response curves, resonance frequencies, and the damping ratios was observed. It can be concluded that the sound field in a cavity containing a bulk-reacting sound absorbing material can be predicted with good accuracy by using BEM.

Acknowledgments

This work was supported, in part, by the National Science Foundation, Grant MSM-8810909. The authors would like to thank C. Y. R. Cheng for the development of an earlier version of the multidomain BEM program and valuable discussions through the course of this work.

References

[1]Dowell, E. H., "Master Plan for Prediction of Vehicle Interior Noise," *AIAA Journal*, Vol. 18, No. 4, 1980, pp. 353–366.

[2]Shuku, T., and Ishihara, K., "The Analysis of the Acoustic Field in Irregularly Shaped Rooms by the Finite Element Method," *Journal of Sound and Vibration*, Vol. 29, No. 1, 1973, pp. 67–76.

[3]Petyt, M., Lea, J., and Koopman, G. H., "A Finite Element Method for Determining the Acoustic Modes of Irregular Shaped Cavities," *Journal of Sound and Vibration*, Vol. 45, No. 4, 1976, pp. 495–502.

[4]Richards, T. L., and Jha, S. K., "A Simplified Finite Element Method for Studying Acoustic Characteristics Inside a Car Cavity," *Journal of Sound and Vibration*, Vol. 63, No. 1, 1979, pp. 61–72.

[5]Nefske, D. J., Wolf, J. A., and Howell, L. J., "Structural-Acoustic Finite Element Analysis of the Automobile Passenger Compartment: A Review of Current Practices," *Journal of Sound and Vibration*, Vol. 80, No. 2, 1982, pp. 247–266.

[6]Ingard, K. U., "Locally and Nonlocally Reacting Flexible Porous Layers; A Comparison of Acoustical Properties," *Journal of Engineering for Industry*, Vol. 103, 1981, pp. 302–313.

[7]Scott, R. A., "The Propagation of Sound Between Walls of Porous Material," *Proceedings of the Physical Society of London*, Vol. 58, 1946, pp. 358–368.

[8]Astley, R. J., and Cummings, A., "A Finite Element Scheme for Attenuation in Ducts Lined with Porous Material: Comparison with Experiment," *Journal of Sound and Vibration*, Vol. 116, No. 2, 1987, pp. 239–263.

[9]Terao, M., and Sekine, H., "On Substructure Boundary Element Techniques to Analyse Acoustic Properties of Air-Duct Component," *Proceedings of Inter-Noise 86*, 1986, pp. 1523–1526.

[10]Seybert, A. F., and Ross, D. F., "Experimental Determination of Acoustic Properties Using a Two Microphone Random Excitation Technique," *Journal of the Acoustical Society of America*, Vol. 61, No. 5, 1977, pp. 1362–1370.

[11]Chung, J. Y., and Blaser, D. A., "Transfer Function Method of Measuring In-Duct Acoustic Properties. I. Theory," *Journal of the Acoustical Society of America*, Vol. 68, No. 3, 1980, pp. 907–913.

[12]Smith, C. D., and Parrott, T. L., "Comparison of Three Methods for Measuring Acoustic Properties of Bulk Materials," *Journal of the Acoustical Society of America*, Vol. 74, No. 5, 1983, pp. 1577–1582.

[13]Craggs, A., "A Finite Element Model for Acoustically Lined Small Rooms," *Journal of Sound and Vibration*, Vol. 108, No. 2, 1986, pp. 327–337.

[14]Bernhard, R. J., Gardner, B. K., and Mollo, C. G., "Prediction of Sound Fields in Cavities Using Boundary-Element Methods," *AIAA Journal*, Vol. 25, No. 9, 1987, pp. 1176–1183.

[15]Utsuno, H., Tanaka, T., Inoue, K., and Nishibe, M., "Analysis of the Sound Field in an Automobile Cabin by Using the Boundary Element Method," Society of Automotive Engineers, Paper 891153, May 1989.

[16]Seybert, A. F., Wu, T. W., and Li, W. L., "Acoustical Prediction for Structural Radiation and Propagation in Automotive Applications," Society of Automotive Engineers, Paper 891169, May 1989.

[17]Suzuki, S., Maruyama, S., and Ido, H., "Boundary Element Analysis of Cavity Noise Problems with Complicated Boundary Conditions," *Journal of Sound and Vibration*, Vol. 130, No. 1, 1989, pp. 79–96.

[18]Cheng, C. Y. R., "Boundary Element Analysis of Single and Multi Domain Problems in Acoustics," Ph.D. Dissertation, University of Kentucky, Lexington, KY, 1988, Chaps. II, V, and VI.

[19]Seybert, A. F., and Wu, T. W. (eds.), *BEMAP User's Manual*, SPECTRONICS, Inc., May 1989.

[20]Utsuno, H., Tanaka, T., Fujikawa, T., and Seybert, A. F., "Transfer Function Method for Measuring Characteristic Impedance and Propagation Constant of Porous Material," *Journal of the Acoustical Society of America*, Vol. 86, No. 2, 1989, pp. 637–643.

[21]Tanaka, T., Fujikawa, T., Abe, T., and Utsuno, H., "A Method for the Analytical Prediction of Insertion Loss of a Two-Dimensional Muffler Model Based on the Transfer Matrix Method Derived from the Boundary Element Method," *Journal of Vibrations, Acoustics, Stress, and Reliability in Design*, Vol. 107, 1985, pp. 86–91.

[22]Seybert, A. F., and Cheng, C. Y. R., "Application of the Boundary Element Method to Acoustic Cavity Response and Muffler Analysis," *Journal of Vibrations, Acoustics, Stress, and Reliability in Design*, Vol. 109, 1987, pp. 15–21.